Adapting a trapped ion mobility spectrometry-Q-TOF mass spectrometer for native mass spectrometry

Yu-Fu Lin,[1,2] Benjamin J. Jones,[3] Mark E. Ridgeway,[3] Erin M. Panczyk,[3] Arpad Somogyi,[1,2] Desmond A. Kaplan,[4] Karen A. Kirby,[5] Stefan G. Sarafianos,[5] Ila Marathe, [1,2] Sangho Yun,[6] Arthur D. Laganowsky,[6] Melvin A. Park,*[3] Vicki Wysocki*[1,2]

1. Department of Chemistry and Biochemistry, The Ohio State University, Columbus, OH

2. Resource for Native MS Guided Structural Biology, The Ohio State University, Columbus, OH

3. Bruker Daltonics Inc., Billerica, MA

4. KapScience LLC, Tewksbury, MA

5. Center for ViroScience and Cure, Laboratory of Biochemical Pharmacology, Department of Pediatrics, Emory University School of Medicine and Children's Healthcare of Atlanta, Atlanta, GA

6. Department of Chemistry, Texas A&M University, College Station, TX

*Corresponding authors: wysocki.11@osu.edu and Mel.Park@bruker.com

Abstract

Native mass spectrometry (nMS) is increasingly popular for studying intact protein quaternary structure. When coupled with ion mobility, which separates ions based on their size, charge, and shape, it provides additional structural information on the protein complex of interest. In this study, we present a novel prototype TIMS (trapped ion mobility spectrometry)-Quadrupole-SID (surface-induced dissociation)-Time of Flight, TIMS-Q-SID-TOF, instrument for nMS. The modifications include changing the TIMS cartridge from concave to convex geometry electrodes and operating TIMS at 425 kHz to improve the trapping efficiency for high mass-to-charge (*m/z*) ion mobility analysis, such as 3 and 4 MDa hepatitis B virus capsids. The quadrupole radiofrequency driver was lowered to 385 kHz, which extends the isolation range from 3,000 to 17,000 *m/z* and allows isolation of a single charge state of GroEL at 16,200 *m/z* with an isolation window of 25 *m/z*. Finally, a 6-mm thick, 2-lens SID device replaced the collision cell entrance lens. SID dissociated 801 kDa GroEL into all combinations of subcomplexes, and the peaks were well-resolved allowing for confident assignment of product ions. This is the first time a novel prototype timsTOF Pro for nMS has been introduced with high resolving power ion mobility separation coupled to high *m/z* quadrupole selection and SID for protein complex fragmentation with product ion collection and detection across a broad *m/z* range of 1,500 to 40,000.

Introduction

Trapped ion mobility spectrometry (TIMS) is a high-resolution ion mobility spectrometry technique that was first introduced by Park and co-workers in 2011.[1,2] Unlike traditional drift tube ion

https://doi.org/10.26434/chemrxiv-2024-xmjml-v3 **ORCID:** https://orcid.org/0000-0003-0476-5193 Content not peer-reviewed by ChemRxiv. **License:** CC BY 4.0

mobility cells (DTIMS), which use ions flying through a stationary gas in the drift tube, TIMS separates ions by using an opposing electric field and a moving column of gas to measure the analyte's ion mobility.[3] TIMS has been coupled to a Q-TOF and FT-ICR mass spectrometer and is widely applied in proteomics and metabolomics, including cross-linking mass spectrometry.[4–8] Recently, Panczyk et al. demonstrated that a commercial TIMS-Q-TOF can perform nMS analysis on protein complexes up to 60 kDa with TIMS.[9] Borotto and co-workers showed that commercial TIMS-Q-TOF could also characterize protein structure up to 66 kDa by top-down sequencing and collision-induced unfolding by activation within the TIMS device.[10,11] Bleiholder and co-workers used and modified tandem TIMS-Q-TOF to characterize the structure of a glycoprotein, avidin, and small proteins.[12,13] Fernandez-Lima and co-workers reported that the modified convex TIMS cartridge with a low radio frequency (RF) driver improves the ion mobility analysis of TIMS up to 800 kDa with a single peak resolution (R_p) of 85 compared to DTIMS with an R_p of 60 for protein complexes around or above 200 kDa.[14–16] Because nMS use is continuing to expand[17–21], and coupling it with IMS provides additional protein and protein complex structural information[22–24], we aimed to adapt TIMS[1–3,25] to perform nMS for studying and understanding large, complex protein structures up to the mega-Dalton (MDa) range with a high energy deposition tandem mass spectrometry (MS/MS) activation method, surface-induced dissociation (SID).[26–29] The Wysocki lab has extended SID development to investigate protein structure and subcomplex connectivity for macromolecules.[27,30–32] SID cleaves protein complexes at their weakest non-covalent interfaces and generates subunits with a charge state approximately proportional to the relative fragment ion mass.[30,33] Currently, nMS has been applied to measure the structures of macromolecules in the MDa mass range, such as adeno-associated virus capsids (3.5 – 5 MDa), antibody-bound capsids species (5 – 17 MDa), and oligomerized 20S proteasome (0.7 – 9.6 MDa), which are important for producing biotherapeutics.[34–37] The Wysocki lab has demonstrated that SID is currently the only activation method capable of extensively dissociating these MDa biomolecules, making it a valuable tool for investigating the structure of AAVs.[38]

Here, we modified a commercial TIMS-Q-TOF mass spectrometer to study the structures of high molecular weight (MW) protein complexes. The modifications include changing the TIMS cartridge geometry to convex, lowering the RF frequency for both the TIMS device and quadrupole, and installing a 2-lens SID device.[39] With these novel modifications, the application of nMS with ion mobility and SID on this prototype platform ranges from 50 kDa to at least 4 MDa.

Experimental Section

Materials and Sample Preparation. More details on materials and selected protein complexes can be found in Supporting Information. All protein complexes were buffer exchanged into 200 mM ammonium acetate using size exclusion chromatography spin columns (Bio-Rad) with a 6 kDa mass cutoff and charge-reduced using 20% (v/v) triethylammonium acetate (TEAA) because we have found that lower charge state precursors of protein complexes give more native-like fragmentation patterns by SID in general.[40] The sample stock solution concentrations were measured using nanoDrop and diluted in the range of 0.7 to 3 µM per complex with or without charge reduction. For T=3 and T=4 hepatitis B virus (HBV) capsids, the concentration was 6 µM per monomer and 4.8 µM per monomer after charge reduction. For the RAS-SOS complex analysis, 3 µM SOS was mixed with 2 µM HRasWT-GTP and immediately introduced into the mass spectrometer via a pulled glass capillary.

Instrumentation and experiments. Experiments were conducted on a timsTOF Pro (TIMS-Q-TOF) (Bruker Inc., Billerica, MA), modified for the research presented here. A 385 kHz RF frequency quadrupole driver was installed to extend the quadrupole isolation range from 3,000 *m/z* with a commercial 1 MHz RF

https://doi.org/10.26434/chemrxiv-2024-xmjml-v3 **ORCID:** https://orcid.org/0000-0003-0476-5193 Content not peer-reviewed by ChemRxiv. **License:** CC BY 4.0

frequency quadrupole driver to 17,000 *m/z*. Here, we used protein complexes for quadrupole calibration up to 12,000 *m/z*, which can isolate a single charge state at 16,200 *m/z* with an isolation width of 25 *m/z* (Figure S1). In general operation, the "TIMS In" pressure was reduced to 2.2 mbar. The "Accumulation time" and "Ramp Time" of the TIMS device were adjusted to 100.0 ms and 1,000.0 ms (10.00 % Duty Cycle), respectively. The "Funnel 1 RF" was 300.0 volt peak-to-peak (V_{pp}). The "Collision Cell In", which determines the *m/z* transferring range, was 150.0 V. The "Pre Pulse Storage", a delay for collecting ions between "Transfer Time" and "TOF Pulser On", was 35.0 µs. The "Transfer Time" is the time corresponding to transmitting ions from the collision cell to the TOF stage and was set to 140.0, 320.0, and 520.0 µs depending on the size of the protein complex. Increasing the "Transfer Time" can transfer larger ions to the TOF. The "Collision Gas Flow Rate" was 35.0 % for the ESI Tuning Mix (Agilent, Santa Clara, CA) and 88.0 % for protein complexes. The default "Delta Values", which control TIMS parameters (Figure S2), was used for all the experiments. More details of the typical settings for nMS can be found in the Supporting Information (Table S1).

All samples were loaded to in-house pulled borosilicate glass capillaries and ionized and introduced using a custom Bruker nanoelectrospray ionization source. The ionization is performed by bringing platinum wire into contact with the sample solution and setting cap voltage to (0.8 – 1.0 kV). The instrument was mass calibrated using ESI Tuning Mix. The SID experiments were conducted with or without single charge state isolation using the quadrupole, as noted in the Results section, and the SID potentials were varied appropriately to initiate the fragmentation of different sizes of chosen analytes (Supporting Information shows the tuning and operation of SID, Table S2 and S3). For pre-ion mobility ion activation experiments, the *Δt6* value was run from 10.0 to 200.0 V.[10,13] The instrument was operated using Bruker's otofControl 6.2 software, and the data were analyzed using DataAnalysis 5.3.

Results and Discussions

To evaluate the performance of the modified instrument (Figure 1), several model protein complexes, including 53 kDa streptavidin (SA), 64 kDa homotetrameric avidin (AV), 103 kDa concanavalin A (Con A), 147 kDa alcohol dehydrogenase (ADH), 58 kDa cholera toxin B (CTB), 115 kDa C-reactive protein (CRP), 90 kDa his-tagged toyocamycin nitrile hydratase (His-TNH), 801 kDa wild-type GroEL, and 3 MDa T=3 and 4 MDa T=4 HBV capsids, were chosen and are discussed below.[30,35,40,41] HRas*GTP-SOS-HRas complex was used to evaluate TIMS-Q-SID performance.[42]

https://doi.org/10.26434/chemrxiv-2024-xmjml-v3 **ORCID:** https://orcid.org/0000-0003-0476-5193 Content not peer-reviewed by ChemRxiv. **License:** CC BY 4.0

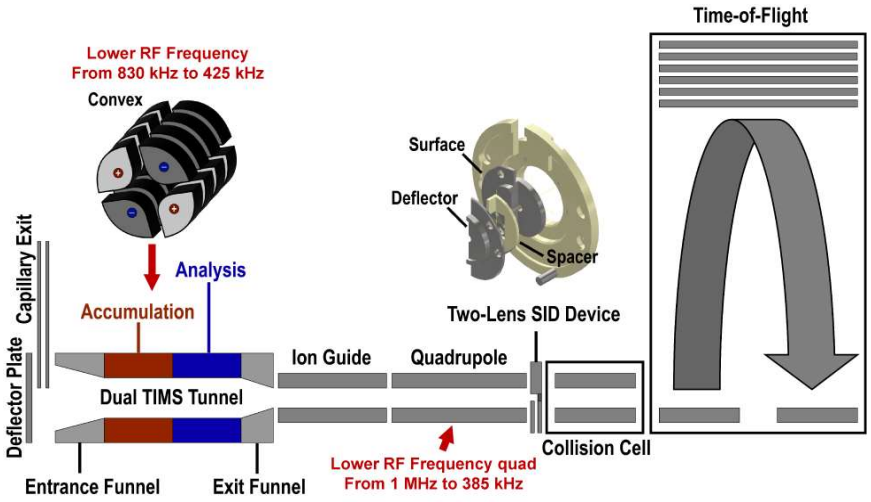

Figure 1. The instrument diagram of the modified Bruker timsTOF Pro. The TIMS cartridge has convex geometry electrodes and is operated at 425 kHz. The quadrupole is operated at 385 kHz to extend the isolation range to 17,000 *m/z*. The 2-lens SID device replaces the entrance lens of the collision cell.

Extending the Mass-to-charge Ratio Range for Protein Complex Ion Mobility Analysis. Initially, the TIMS-Q-TOF instrument was configured with a concave TIMS cartridge (Figure S3a) with an 830 kHz RF TIMS driver, which can trap ions up to 6,000 *m/z*.[9] In the work described here, the TIMS cartridge was changed to a convex electrode geometry (inset of Figure 1 and Figure S3b) coupled with a 425 kHz RF frequency TIMS driver to enhance the trapping efficiency for species up to 38,000 *m/z*. The performance of the TIMS device with convex electrodes was verified with selected model protein complexes, which ranged in mass from 50 – 801 kDa (4,500 – 18,500 *m/z*).

To test the effective *m/z* range of this modified TIMS device, lower-mass complexes and 180-mer T=3 and 240-mer T=4 HBV capsids, with masses of ~3 MDa and ~4 MDa, respectively, were investigated.[35,43] The mobility peaks for different charge states of lower-mass complexes, SA and ADH, were mostly baseline resolved (Figure S4). Figure 2a shows the MS spectrum of T=3 and T=4 HBV. With the modified TIMS cartridge, T=3 and T=4 capsids were trapped successfully during the ion mobility analysis (Figure 2b). The *m/z* peaks of each distribution are partially resolved, and the charge states of the central distribution of each HBV capsid can be determined. T=3 and T=4 capsids were also further charge-reduced with TEAA, and the result is shown in Figure S5. We were still able to trap the charge-reduced T=3 and T=4 capsids (28,000 – 39,000 *m/z*), determine their approximate charge state, and separate the overlapped species using this modified TIMS device (Figure S6).

https://doi.org/10.26434/chemrxiv-2024-xmjml-v3 **ORCID:** https://orcid.org/0000-0003-0476-5193 Content not peer-reviewed by ChemRxiv. **License:** CC BY 4.0

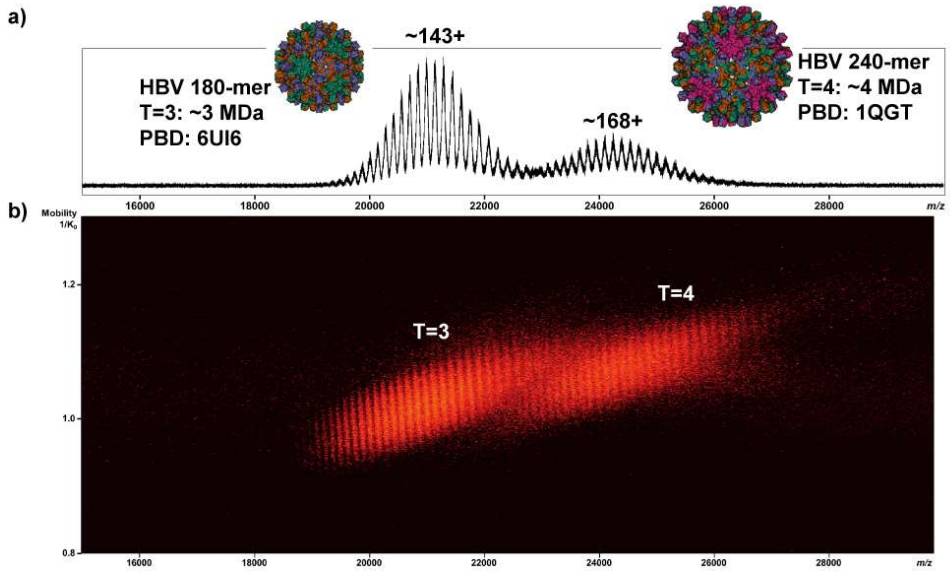

Figure 2. a) The spectrum of ~33 nM 180-mer (T=3, ~3 MDa) and ~25 nM 240-mer (T=4, ~4 MDa) HBV capsids (~ 6 µM per monomer) in 200 mM ammonium acetate. b) The mobiligram of T=3 and T=4 capsids. The modified TIMS cartridge trapped both T=3 and T=4 capsids and measured their ion mobilities.

Performance of a Two-lens Surface-induced Dissociation Device. The SID device design on this instrument was inspired by the designs of Snyder et al.[39] The device is simplified to a 2-lens system (inset of Figure 1). The overall width of this device along the ion optical axis is 6 mm, which is the width of the collision cell entrance lens that was removed. The SID surface and extractor were combined into a ring electrode with a 3 mm diameter aperture. The deflector is a half-moon-shaped electrode. Both surface and deflector were made with tight-tolerance corrosion-resistant 316 stainless steel. An insulated spacer made of polyether ether ketone (PEEK) material was placed between the surface and the deflector to prevent an electrical short circuit. The surface was controlled by an existing spare system voltage on the instrument, and the deflector was controlled using the voltage typically supplied to the collision cell entrance lens (Focus 2 L3). To examine the performance of the installed SID device, selected homotetrameric (SA, AV, ADH, ConA) and homopentameric (CTB and CRP) model protein complexes and heterohexameric His-TNH were fragmented by SID, and results are shown in Figure 3.

https://doi.org/10.26434/chemrxiv-2024-xmjml-v3 **ORCID:** https://orcid.org/0000-0003-0476-5193 Content not peer-reviewed by ChemRxiv. **License:** CC BY 4.0

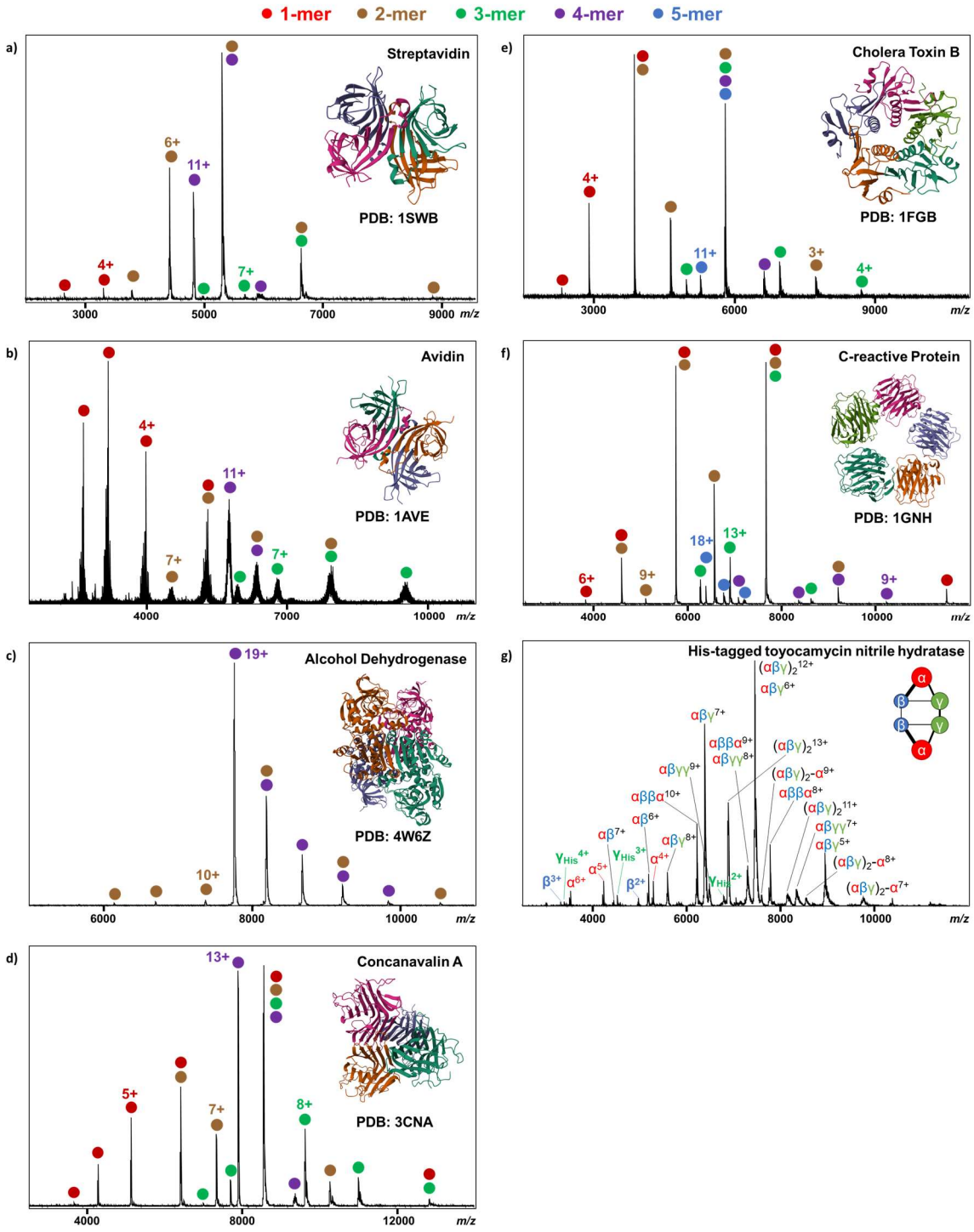

Figure 3. SID spectra of a) 11+ streptavidin at SID 440 eV, b) 11+ avidin at SID 880 eV, c) 19+ alcohol dehydrogenase at SID 3,040 eV, d) 13+ concanavalin A at SID 1,105 eV, e) 11+ cholera toxin B at SID 880 eV, f) 18+ C-reactive protein at SID 1,080 eV, and g) 13+ His-tagged toyocamycin nitrile hydratase at SID 1,170 eV. The results were consistent with the reported data.[30,44,45] Monomers, dimers, trimers, tetramers, and pentamers are represented by red, brown, green, purple, and blue dots, respectively.

https://doi.org/10.26434/chemrxiv-2024-xmjml-v3 **ORCID:** https://orcid.org/0000-0003-0476-5193 Content not peer-reviewed by ChemRxiv. **License:** CC BY 4.0

The largest protein complex fragmented here to test the SID performance was 14-mer 801 kDa GroEL, normal charge in 200 mM ammonium acetate and charge-reduced species using TEAA (Figure S7). We isolated 68+ and 47+ GroEL at 11,850 and 16,950 *m/z*, respectively, with an isolation window of 200 *m/z* using quadrupole, and fragmented them using SID. The SID energies were adjusted to 7,520 eV and 7,480 eV, respectively, to compare their results under an approximately equal SID energy level. Figure 4 shows the SID results from both selected ions. After deconvolving the spectrum using UniDec[46], the results show that, after SID, 47+ GroEL (Figure 4d) has fewer monomers and 13-mers formed, and it is more favorable to produce 7-mers, which reflects a more native-like structure compared to the SID result of 68+ GroEL (Figure 4b).

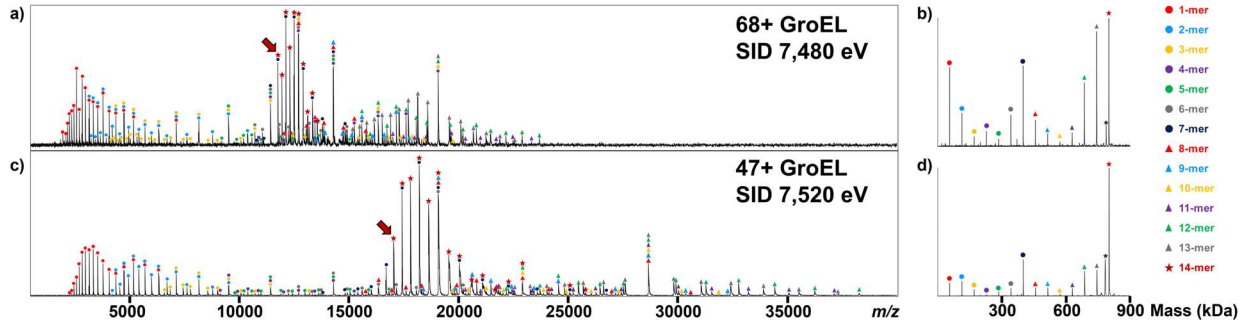

Figure 4. The SID spectra of a) 68+ and c) 47+ GroEL at SID energy 7,480 and 7,520 eV, respectively. The deconvolved mass spectra show the relative abundance of SID products from b) 68+ and d) 47+ GroEL. The red arrows indicate the selected 68+ and 47+ GroEL precursors. The legend shows different subcomplexes of GroEL SID products and their representative symbols. The asterisk represents a deconvolution error. These deconvolution error peaks are assigned from an atypical *m/z* peak distribution (asymmetric peak heights from the centroid peak).

Analysis of a complex mixture using the modified TIMS-Q-TOF. When the sample is a complex mixture, sometimes the protein complex of interest can overlap with others under the same *m/z*. Using TIMS to separate the mixture by ion mobility (IM) and isolating a narrow *m/z* range of interest before SID makes the identification of SID fragments easier. GTPase, Ras, is a key component of the mitogen-activated protein kinase signaling pathway, cycling between guanosine diphosphate-bound inactive and guanosine triphosphate (GTP)-bound active states.[47] It forms a complex with a specific guanine nucleotide exchange factor, Son of Sevenless (SOS). Ras*GTP binds at the distal site, which modulates the activity of SOS, while Ras binds at the active site, facilitating nucleotide exchange.[42,48] To investigate the HRas-SOS complex structure, HRas*GTP and SOS were mixed and ionized and 4 different proteins and protein complexes, HRas*GTP, SOS, HRas*GTP-SOS, and HRas*GTP-SOS-HRas, were observed in the MS1 spectrum (Figure 5a). We were interested in studying the structure of the full HRas*GTP-SOS-HRas complex. However, from the mobiligram shown in Figure 5b, there were always other protein complexes and overlapped HRas*GTP-SOS-HRas in *m/z*. Those overlapped protein complexes, which could not be separated without IM or by narrowing the *m/z* range using quadrupole, were also fragmented when performing MS/MS on HRas*GTP-SOS-HRas. Therefore, using TIMS to separate overlapped species prior to quadrupole isolation and MS/MS can improve the structure analysis of the HRas*GTP-SOS-HRas complex.

To perform SID and characterize the HRas*GTP-SOS-HRas complex, the mixture was first separated using TIMS. We then isolated a narrow *m/z* range of interest, and 16+ HRas*GTP-SOS and 20+ HRas*GTP-SOS-HRas were isolated. These two complexes were then fragmented by SID. To identify the SID fragments of 20+ HRas*GTP-SOS-HRas, we generated the SID spectrum of 20+ HRas*GTP-SOS-HRas

https://doi.org/10.26434/chemrxiv-2024-xmjml-v3 **ORCID:** https://orcid.org/0000-0003-0476-5193 Content not peer-reviewed by ChemRxiv. **License:** CC BY 4.0

by extracting its mobility peak (Figure 5c). The result shows that HRas*GTP-SOS-HRas dissociates into two species: HRas and HRas*GTP-SOS, and HRas*GTP retains on SOS after SID. This indicates that HRas*GTP binds more strongly with SOS than HRas. It's also interesting to note that HRas carried about half of the charges from the precursor after being dissociated from the complex, which was not anticipated. Typically, SID fragments carry charges proportional to the mass of the precursor.[27,29,32] This suggests that HRas undergoes structural rearrangement to depart from the complex, which is similar to results reported for some other complexes.[49] To understand the effect of GTP on HRas' structure stability, further study is required. Overall, by combining TIMS separation and quadrupole isolation, we were able to study the structure of HRas*GTP-SOS-HRas using SID without any interference from other complexes in the mixture.

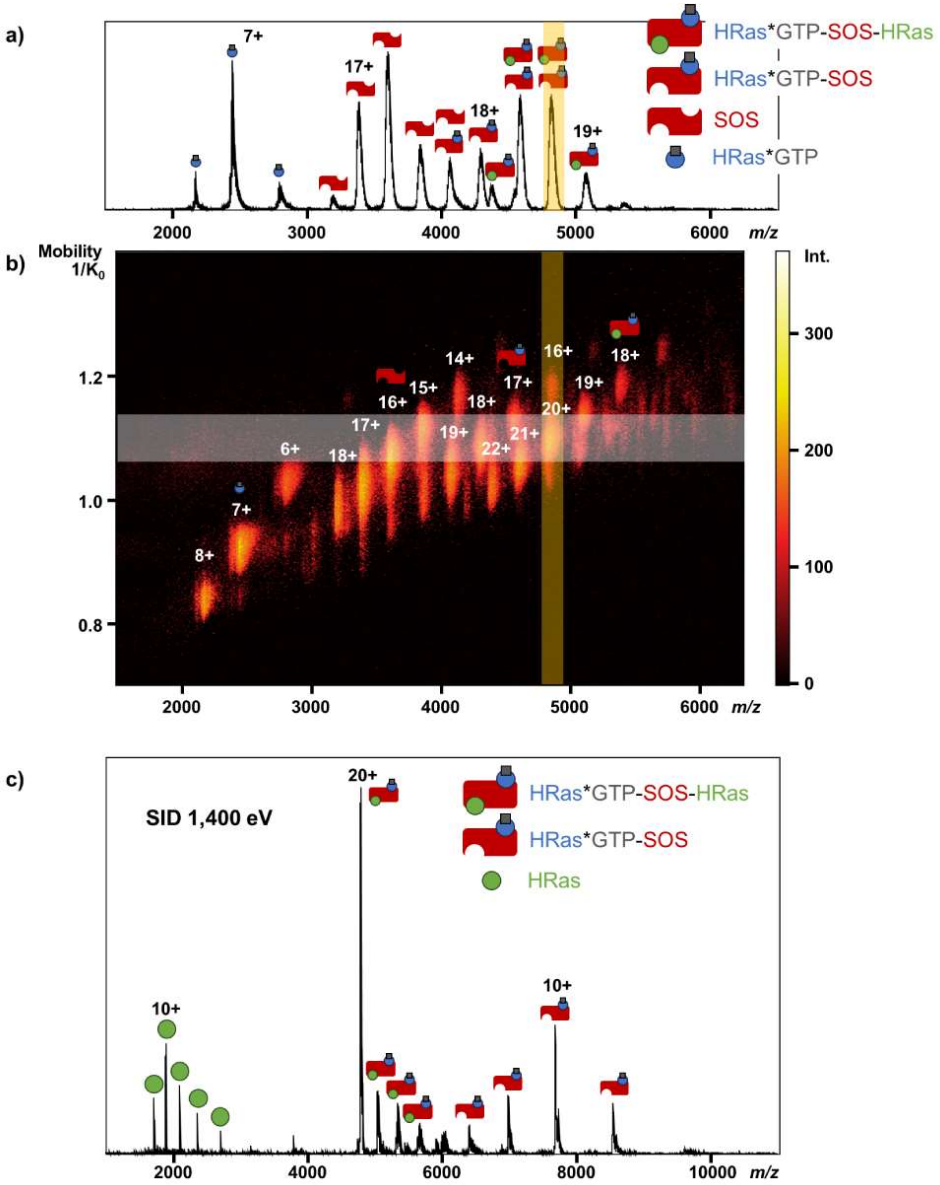

Figure 5 a) The mass spectrum and b) the mobiligram of the HRas-SOS complex. c) The SID result of 20+ HRas*GTP-SOS-HRas at SID 1,400 eV. The shaded yellow area represents the isolation using quadrupoles,

https://doi.org/10.26434/chemrxiv-2024-xmjml-v3 **ORCID:** https://orcid.org/0000-0003-0476-5193 Content not peer-reviewed by ChemRxiv. **License:** CC BY 4.0

while the white area represents the extracting mobility area (1.07 – 1.11 $1/K_0$) used to generate the SID spectrum after quadrupole isolating at 4,800 *m/z* with a width of 100 *m/z*.

Conclusions

Here, we demonstrated that with a low RF frequency convex TIMS device, we are able to mobility-separate charge-reduced 3 and 4 MDa T=3 and T=4 HBV capsids. A single charge state of charge-reduced GroEL could be selected at *m/z* 16,200 with a 25 *m/z* isolation window with the low RF frequency quadrupole driver. Also, a 2-lens SID device was able to fragment 801 kDa GroEL and investigate its subunit connectivity. Significantly, the peaks of fragments at high *m/z* are well resolved, which improves the identification of different subcomplexes. SID can also be used as a tool to probe the structural information of ions of interest. The detection limit of this instrument is also outstanding. We were able to perform nMS for HBV capsids in the concentration range of 20 to 50 nM. Moreover, with TIMS, when characterizing a specific protein complex from a complex mixture using nMS, we were able to differentiate those SID fragments from others. This simplifies the interpretation of SID products from the complex mixture.

Supporting Information

Additional materials, instrument parameters, SID operation, supporting figures of the mass spectra of isolated 49+ GroEL, diagram of the TIMS device, electrode geometry of concave and convex TIMS cartridges, mass spectra of streptavidin and alcohol dehydrogenase and their extracted mobility peaks, charge-reduced T3 and T4 HBV mass spectrum and mobiligrams, and SID spectra of selected model protein complexes.

Author Information

The authors declare the following competing financial interests: BJJ, MER, EMP, and MAP are employees of Bruker, which manufactures and sells the Bruker timsTOF Pro modified in this work. The work in the Wysocki lab was performed collaboratively with the Bruker team.

Acknowledgments

We thank Dalton T. Snyder (Resource for Native Mass Spectrometry Guided Structural Biology, OSU) for helpful discussions, Marshell Bern and Ignat Shilov (Protein Metrics, LLC) for the input and discussion of the deconvolved GroEL SID results, and the Ohio State University ASC machine shop for machining SID device parts. We also thank Bandarian lab (University of Utah) for his-tagged toyocamycin nitrile hydratase, and the Hayes Rye Group (Texas A&M University) for wild-type GroEL samples. We gratefully acknowledge funding from the National Institutes of Health (NIH RM1GM149374 to V. H. W., U54AI170855 to S. G. S, and R01AI132833 to S. G. S.).

Reference

(1) Fernandez-Lima, F.; Kaplan, D. A.; Suetering, J.; Park, M. A. Gas-Phase Separation Using a Trapped Ion Mobility Spectrometer. *Int. J. Ion Mobil. Spec.* **2011**, *14* (2), 93–98. https://doi.org/10.1007/s12127-011-0067-8.

https://doi.org/10.26434/chemrxiv-2024-xmjml-v3 **ORCID:** https://orcid.org/0000-0003-0476-5193 Content not peer-reviewed by ChemRxiv. **License:** CC BY 4.0

(2) Fernandez-Lima, F. A.; Kaplan, D. A.; Park, M. A. Note: Integration of Trapped Ion Mobility Spectrometry with Mass Spectrometry. *Review of Scientific Instruments* **2011**, *82* (12), 126106. https://doi.org/10.1063/1.3665933.
(3) Ridgeway, M. E.; Lubeck, M.; Jordens, J.; Mann, M.; Park, M. A. Trapped Ion Mobility Spectrometry: A Short Review. *International Journal of Mass Spectrometry* **2018**, *425*, 22–35. https://doi.org/10.1016/j.ijms.2018.01.006.
(4) Ridgeway, M. E.; Bleiholder, C.; Mann, M.; Park, M. A. Trends in Trapped Ion Mobility – Mass Spectrometry Instrumentation. *TrAC Trends in Analytical Chemistry* **2019**, *116*, 324–331. https://doi.org/10.1016/j.trac.2019.03.030.
(5) Meier, F.; Park, M. A.; Mann, M. Trapped Ion Mobility Spectrometry and Parallel Accumulation–Serial Fragmentation in Proteomics. *Molecular & Cellular Proteomics* **2021**, *20*. https://doi.org/10.1016/j.mcpro.2021.100138.
(6) Ihling, C. H.; Piersimoni, L.; Kipping, M.; Sinz, A. Cross-Linking/Mass Spectrometry Combined with Ion Mobility on a TimsTOF Pro Instrument for Structural Proteomics. *Anal. Chem.* **2021**, *93* (33), 11442–11450. https://doi.org/10.1021/acs.analchem.1c01317.
(7) Panczyk, E. M.; Snyder, D. T.; Ridgeway, M. E.; Somogyi, Á.; Park, M. A.; Wysocki, V. H. Surface-Induced Dissociation of Protein Complexes Selected by Trapped Ion Mobility Spectrometry. *Anal. Chem.* **2021**, *93* (13), 5513–5520. https://doi.org/10.1021/acs.analchem.0c05373.
(8) Guergues, J.; Wohlfahrt, J.; Stevens, S. M. Jr. Enhancement of Proteome Coverage by Ion Mobility Fractionation Coupled to PASEF on a TIMS–QTOF Instrument. *J. Proteome Res.* **2022**, *21* (8), 2036–2044. https://doi.org/10.1021/acs.jproteome.2c00336.
(9) Panczyk, E.; Lin, Y.-F.; Snyder, D.; Liu, F.; Ridgeway, M.; Park, M.; Bleiholder, C.; Wysocki, V. Evaluation of a Bruker TimsTOF Pro for Native Mass Spectrometry. ChemRxiv September 12, 2023. https://doi.org/10.26434/chemrxiv-2021-qr78t-v2.
(10) Borotto, N. B.; Osho, K. E.; Richards, T. K.; Graham, K. A. Collision-Induced Unfolding of Native-like Protein Ions Within a Trapped Ion Mobility Spectrometry Device. *J. Am. Soc. Mass Spectrom.* **2022**, *33* (1), 83–89. https://doi.org/10.1021/jasms.1c00273.
(11) Graham, K. A.; Lawlor, C. F.; Borotto, N. B. Characterizing the Top-down Sequencing of Protein Ions Prior to Mobility Separation in a TimsTOF. *Analyst* **2023**, *148* (7), 1534–1542. https://doi.org/10.1039/d2an01682f.
(12) Liu, F. C.; Cropley, T. C.; Ridgeway, M. E.; Park, M. A.; Bleiholder, C. Structural Analysis of the Glycoprotein Complex Avidin by Tandem-Trapped Ion Mobility Spectrometry–Mass Spectrometry (Tandem-TIMS/MS). *Anal. Chem.* **2020**, *92* (6), 4459–4467. https://doi.org/10.1021/acs.analchem.9b05481.
(13) Liu, F. C.; Ridgeway, M. E.; Winfred, J. S. R. V.; Polfer, N. C.; Lee, J.; Theisen, A.; Wootton, C. A.; Park, M. A.; Bleiholder, C. Tandem-Trapped Ion Mobility Spectrometry/Mass Spectrometry Coupled with Ultraviolet Photodissociation. *Rapid Communications in Mass Spectrometry* **2021**, *35* (22), e9192. https://doi.org/10.1002/rcm.9192.
(14) McCabe, J. W.; Mallis, C. S.; Kocurek, K. I.; Poltash, M. L.; Shirzadeh, M.; Hebert, M. J.; Fan, L.; Walker, T. E.; Zheng, X.; Jiang, T.; Dong, S.; Lin, C.-W.; Laganowsky, A.; Russell, D. H. First-Principles Collision Cross Section Measurements of Large Proteins and Protein Complexes. *Anal Chem* **2020**, *92* (16), 11155–11163. https://doi.org/10.1021/acs.analchem.0c01285.
(15) France, A. P.; Migas, L. G.; Sinclair, E.; Bellina, B.; Barran, P. E. Using Collision Cross Section Distributions to Assess the Distribution of Collision Cross Section Values. *Anal. Chem.* **2020**, *92* (6), 4340–4348. https://doi.org/10.1021/acs.analchem.9b05130.

https://doi.org/10.26434/chemrxiv-2024-xmjml-v3 **ORCID:** https://orcid.org/0000-0003-0476-5193 Content not peer-reviewed by ChemRxiv. **License:** CC BY 4.0

(16) Jeanne Dit Fouque, K.; Garabedian, A.; Leng, F.; Tse-Dinh, Y.-C.; Ridgeway, M. E.; Park, M. A.; Fernandez-Lima, F. Trapped Ion Mobility Spectrometry of Native Macromolecular Assemblies. *Anal. Chem.* **2021**, *93* (5), 2933–2941. https://doi.org/10.1021/acs.analchem.0c04556.
(17) Zhou, M.; Lantz, C.; A. Brown, K.; Ge, Y.; Paša-Tolić, L.; A. Loo, J.; Lermyte, F. Higher-Order Structural Characterisation of Native Proteins and Complexes by Top-down Mass Spectrometry. *Chemical Science* **2020**, *11* (48), 12918–12936. https://doi.org/10.1039/D0SC04392C.
(18) Ruotolo, B. T.; Marty, M. T. Native Mass Spectrometry for Structural Biology: A Perspective. *International Journal of Mass Spectrometry* **2021**, *468*, 116655. https://doi.org/10.1016/j.ijms.2021.116655.
(19) Campuzano, I. D. G.; Sandoval, W. Denaturing and Native Mass Spectrometric Analytics for Biotherapeutic Drug Discovery Research: Historical, Current, and Future Personal Perspectives. *J. Am. Soc. Mass Spectrom.* **2021**, *32* (8), 1861–1885. https://doi.org/10.1021/jasms.1c00036.
(20) Tamara, S.; den Boer, M. A.; Heck, A. J. R. High-Resolution Native Mass Spectrometry. *Chem. Rev.* **2022**, *122* (8), 7269–7326. https://doi.org/10.1021/acs.chemrev.1c00212.
(21) Rolland, A. D.; Prell, J. S. Approaches to Heterogeneity in Native Mass Spectrometry. *Chem. Rev.* **2022**, *122* (8), 7909–7951. https://doi.org/10.1021/acs.chemrev.1c00696.
(22) Konijnenberg, A.; Butterer, A.; Sobott, F. Native Ion Mobility-Mass Spectrometry and Related Methods in Structural Biology. *Biochimica et Biophysica Acta (BBA) - Proteins and Proteomics* **2013**, *1834* (6), 1239–1256. https://doi.org/10.1016/j.bbapap.2012.11.013.
(23) Allison, T. M.; Barran, P.; Cianférani, S.; Degiacomi, M. T.; Gabelica, V.; Grandori, R.; Marklund, E. G.; Menneteau, T.; Migas, L. G.; Politis, A.; Sharon, M.; Sobott, F.; Thalassinos, K.; Benesch, J. L. P. Computational Strategies and Challenges for Using Native Ion Mobility Mass Spectrometry in Biophysics and Structural Biology. *Anal. Chem.* **2020**, *92* (16), 10872–10880. https://doi.org/10.1021/acs.analchem.9b05791.
(24) McCabe, J. W.; Hebert, M. J.; Shirzadeh, M.; Mallis, C. S.; Denton, J. K.; Walker, T. E.; Russell, D. H. The Ims Paradox: A Perspective on Structural Ion Mobility-Mass Spectrometry. *Mass Spectrometry Reviews* **2021**, *40* (3), 280–305. https://doi.org/10.1002/mas.21642.
(25) Ridgeway, M.; Woods, L.; Park, M. CHAPTER 5:Trapped Ion Mobility Spectrometry – Basics and Calibration. In *Ion Mobility-Mass Spectrometry*; 2021; pp 105–131. https://doi.org/10.1039/9781839162886-00105.
(26) Morris, M. R.; Riederer, D. E.; Winger, B. E.; Cooks, R. G.; Ast, T.; Chidsey, C. E. D. Ion/Surface Collisions at Functionalized Self-Assembled Monolayer Surfaces. *International Journal of Mass Spectrometry and Ion Processes* **1992**, *122*, 181–217. https://doi.org/10.1016/0168-1176(92)87016-8.
(27) Stiving, A. Q.; VanAernum, Z. L.; Busch, F.; Harvey, S. R.; Sarni, S. H.; Wysocki, V. H. Surface-Induced Dissociation: An Effective Method for Characterization of Protein Quaternary Structure. *Anal. Chem.* **2019**, *91* (1), 190–209. https://doi.org/10.1021/acs.analchem.8b05071.
(28) Snyder, D. T.; Harvey, S. R.; Wysocki, V. H. Surface-Induced Dissociation Mass Spectrometry as a Structural Biology Tool. *Chem. Rev.* **2021**, acs.chemrev.1c00309. https://doi.org/10.1021/acs.chemrev.1c00309.
(29) Karch, K. R.; Snyder, D. T.; Harvey, S. R.; Wysocki, V. H. Native Mass Spectrometry: Recent Progress and Remaining Challenges. *Annual Review of Biophysics* **2022**, *51* (1), null. https://doi.org/10.1146/annurev-biophys-092721-085421.
(30) Harvey, S. R.; Seffernick, J. T.; Quintyn, R. S.; Song, Y.; Ju, Y.; Yan, J.; Sahasrabuddhe, A. N.; Norris, A.; Zhou, M.; Behrman, E. J.; Lindert, S.; Wysocki, V. H. Relative Interfacial Cleavage Energetics of Protein Complexes Revealed by Surface Collisions. *PNAS* **2019**, *116* (17), 8143–8148. https://doi.org/10.1073/pnas.1817632116.

https://doi.org/10.26434/chemrxiv-2024-xmjml-v3 **ORCID:** https://orcid.org/0000-0003-0476-5193 Content not peer-reviewed by ChemRxiv. **License:** CC BY 4.0

(31) Harvey, S. R.; Liu, Y.; Liu, W.; Wysocki, V. H.; Laganowsky, A. Surface Induced Dissociation as a Tool to Study Membrane Protein Complexes. *Chem. Commun.* **2017**, *53* (21), 3106–3109. https://doi.org/10.1039/C6CC09606A.
(32) Snyder, D. T.; Jones, B. J.; Lin, Y.-F.; Cooper-Shepherd, D. A.; Hewitt, D.; Wildgoose, J.; Brown, J. M.; Langridge, J. I.; Wysocki, V. H. Surface-Induced Dissociation of Protein Complexes on a Cyclic Ion Mobility Spectrometer. *Analyst* **2021**, *146* (22), 6861–6873. https://doi.org/10.1039/D1AN01407B.
(33) Wang, J.; Meroueh, S. O.; Wang, Y.; Hase, W. L. Efficiency of Energy Transfer in Protonated Diglycine and Dialanine SID: Effects of Collision Angle, Peptide Ion Size, and Intramolecular Potential. *International Journal of Mass Spectrometry* **2003**, *230* (1), 57–63. https://doi.org/10.1016/j.ijms.2003.08.005.
(34) Barnes, L. F.; Draper, B. E.; Jarrold, M. F. Analysis of Recombinant Adenovirus Vectors by Ion Trap Charge Detection Mass Spectrometry: Accurate Molecular Weight Measurements beyond 150 MDa. *Anal. Chem.* **2022**, *94* (3), 1543–1551. https://doi.org/10.1021/acs.analchem.1c02439.
(35) Uetrecht, C.; Versluis, C.; Watts, N. R.; Roos, W. H.; Wuite, G. J. L.; Wingfield, P. T.; Steven, A. C.; Heck, A. J. R. High-Resolution Mass Spectrometry of Viral Assemblies: Molecular Composition and Stability of Dimorphic Hepatitis B Virus Capsids. *Proceedings of the National Academy of Sciences* **2008**, *105* (27), 9216–9220. https://doi.org/10.1073/pnas.0800406105.
(36) Grande, A. E.; Li, X.; Miller, L. M.; Zhang, J.; Draper, B. E.; Herzog, R. W.; Xiao, W.; Jarrold, M. F. Antibody Binding to Recombinant Adeno Associated Virus Monitored by Charge Detection Mass Spectrometry. *Anal. Chem.* **2023**, *95* (29), 10864–10868. https://doi.org/10.1021/acs.analchem.3c02371.
(37) Anthony, A. J.; Gautam, A. K. S.; Miller, L. M.; Ma, Y.; Hardwick, A. G.; Sharma, A.; Ghatak, S.; Matouschek, A.; Jarrold, M. F.; Clemmer, D. E. CDMS Analysis of Intact 19S, 20S, 26S, and 30S Proteasomes: Evidence for Higher-Order 20S Assemblies at a Low PH. *Anal. Chem.* **2023**, *95* (33), 12209–12215. https://doi.org/10.1021/acs.analchem.3c00472.
(38) Du, C.; Cleary, S. P.; Kostelic, M. M.; Jones, B. J.; Kafader, J. O.; Wysocki, V. H. Combining Surface-Induced Dissociation and Charge Detection Mass Spectrometry to Reveal the Native Topology of Heterogeneous Protein Complexes. *Anal. Chem.* **2023**, *95* (37), 13889–13896. https://doi.org/10.1021/acs.analchem.3c02185.
(39) Snyder, D. T.; Panczyk, E. M.; Somogyi, A.; Kaplan, D. A.; Wysocki, V. Simple and Minimally Invasive SID Devices for Native Mass Spectrometry. *Anal. Chem.* **2020**, *92* (16), 11195–11203. https://doi.org/10.1021/acs.analchem.0c01657.
(40) Zhou, M.; Jones, C. M.; Wysocki, V. H. Dissecting the Large Noncovalent Protein Complex GroEL with Surface-Induced Dissociation and Ion Mobility–Mass Spectrometry. *Anal. Chem.* **2013**, *85* (17), 8262–8267. https://doi.org/10.1021/ac401497c.
(41) Quintyn, R. S.; Zhou, M.; Yan, J.; Wysocki, V. H. Surface-Induced Dissociation Mass Spectra as a Tool for Distinguishing Different Structural Forms of Gas-Phase Multimeric Protein Complexes. *Anal. Chem.* **2015**, *87* (23), 11879–11886. https://doi.org/10.1021/acs.analchem.5b03441.
(42) Yun, S. D.; Scott, E.; Moghadamchargari, Z.; Laganowsky, A. 2′-Deoxy Guanosine Nucleotides Alter the Biochemical Properties of Ras. *Biochemistry* **2023**, *62* (16), 2450–2460. https://doi.org/10.1021/acs.biochem.3c00258.
(43) Uetrecht, C.; Barbu, I. M.; Shoemaker, G. K.; van Duijn, E.; Heck, A. J. R. Interrogating Viral Capsid Assembly with Ion Mobility-Mass Spectrometry. *Nat Chem* **2011**, *3* (2), 126–132. https://doi.org/10.1038/nchem.947.
(44) Quintyn, R. S.; Yan, J.; Wysocki, V. H. Surface-Induced Dissociation of Homotetramers with D2 Symmetry Yields Their Assembly Pathways and Characterizes the Effect of Ligand Binding. *Chemistry & Biology* **2015**, *22* (5), 583–592. https://doi.org/10.1016/j.chembiol.2015.03.019.

https://doi.org/10.26434/chemrxiv-2024-xmjml-v3 **ORCID:** https://orcid.org/0000-0003-0476-5193 Content not peer-reviewed by ChemRxiv. **License:** CC BY 4.0

(45) Snyder, D. T.; Lin, Y.-F.; Somogyi, A.; Wysocki, V. H. Tandem Surface-Induced Dissociation of Protein Complexes on an Ultrahigh Resolution Platform. *International Journal of Mass Spectrometry* **2021**, *461*, 116503. https://doi.org/10.1016/j.ijms.2020.116503.
(46) Kostelic, M. M.; Zak, C. K.; Liu, Y.; Chen, V. S.; Wu, Z.; Sivinski, J.; Chapman, E.; Marty, M. T. UniDecCD: Deconvolution of Charge Detection-Mass Spectrometry Data. *Anal. Chem.* **2021**, *93* (44), 14722–14729. https://doi.org/10.1021/acs.analchem.1c03181.
(47) Goitre, L.; Trapani, E.; Trabalzini, L.; Retta, S. F. The Ras Superfamily of Small GTPases: The Unlocked Secrets. In *Ras Signaling: Methods and Protocols*; Trabalzini, L., Retta, S. F., Eds.; Humana Press: Totowa, NJ, 2014; pp 1–18. https://doi.org/10.1007/978-1-62703-791-4_1.
(48) Moghadamchargari, Z.; Shirzadeh, M.; Liu, C.; Schrecke, S.; Packianathan, C.; Russell, D. H.; Zhao, M.; Laganowsky, A. Molecular Assemblies of the Catalytic Domain of SOS with KRas and Oncogenic Mutants. *Proc Natl Acad Sci U S A* **2021**, *118* (12), e2022403118. https://doi.org/10.1073/pnas.2022403118.
(49) Sahasrabuddhe, A.; Hsia, Y.; Busch, F.; Sheffler, W.; King, N. P.; Baker, D.; Wysocki, V. H. Confirmation of Intersubunit Connectivity and Topology of Designed Protein Complexes by Native MS. *Proceedings of the National Academy of Sciences* **2018**, *115* (6), 1268–1273. https://doi.org/10.1073/pnas.1713646115.

For Table of Contents Only

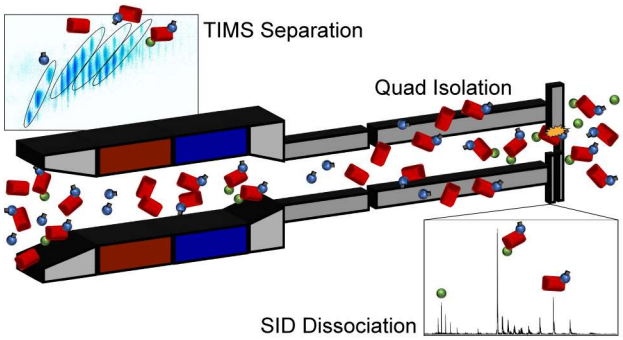

https://doi.org/10.26434/chemrxiv-2024-xmjml-v3 **ORCID:** https://orcid.org/0000-0003-0476-5193 Content not peer-reviewed by ChemRxiv. **License:** CC BY 4.0